An Integrated Charger for Plug-in Hybrid Electric Vehicles Based on a Special Interior Permanent Magnet Motor

Saeid Haghbin*, Mats Alakula†, Kashif Khan‡, Sonja Lundmark*, Mats Leksell‡, Oskar Wallmark‡ and Ola Carlson*
*Electric Power Engineering Division of Chalmers University of Technology, Sweden
†Department of Industrial Electrical Engineering, Lund University, Sweden
‡Electrical Machines & Drives of Royal Institute of Technology, Sweden
E-mail: saeid.haghbin@chalmers.se

***Abstract*—For a plug-in hybrid electric vehicle (PHEV), the battery needs to be charged from the grid while the vehicle is parked. The traction system components are normally not engaged during the charging time so there is a possibility to use them in the charger system to develop an integrated charger. An innovative high power isolated three-phase bi-directional integrated charger with unit power factor operation is introduced for PHEVs based on a special configuration of the ac motor. The winding of the machine is re-arranged in charging mode to have a three-phase boost based high power battery charger. The system configuration, the device model (machine with multiple windings), traction and charging system functionality and charger control are presented in this paper.**

I. Introduction

An on-board battery charger is an interesting option for PHEV (or EV) users since that allows them to charge their vehicles everywhere that a suitable power source is available. With requirements on galvanic isolation and 3-phase connection for high power charging the weight and cost of a separate on board charging system becomes unrealistically high. If the traction and charging are not happening in the same time, it is possible to use the traction system components, like inverter and motor, in the charger system to have an integrated charging device with reduced weight, space and in total cost. Several integrated chargers in vehicle applications have been reported by the academia or industry (see references in [1]).

An innovative integrated charger is proposed in this paper based on a special electrical machine design and configuration. Contrary to other solutions mentioned in [1], this is an isolated high power three-phase bi-directional integrated charger with unit power factor operation capability. Accordingly, an interior permanent magnet synchronous motor (IPMSM) is designed [2] with a special winding configuration with two functions: motor operation in traction mode and assistance of charging in the charging mode. Depending on the desired mode of operation the system hardware will be reconfigured for the traction or charging operation. The traction-mode inverter acts like a rectifier in the charging mode.

The system mode of operation in charging and traction is described first. Afterwards, the mathematical model of the IPMSM motor with double stator windings is presented. The grid synchronization and charging control are described also. Moreover, simulation results of the system for the charging mode will be presented.

II. Integrated charger based on a special motor configuration

Fig. 1 shows a schematic diagram of a PHEV with a parallel configuration [3]. The electrical part includes the grid connected battery charger, battery, inverter, motor and control system. During charging time the vehicle is not driven and during driving time it is not intended to charge the battery pack except for regeneration at braking. However, it is possible to integrate both hardware to use the inverter and motor in the charger circuit to reduce the system components, space and weight which is equivalent to the cost reduction. This is what is referred to as an integrated charger in this paper.

The main idea is to introduce a multi terminal device called motor/generator set to act like a motor in the traction mode and an isolated generator/transformer in the charging mode. With this scheme the separate battery charger will be eliminated from the system. The inverter, motor with re-configured stator windings and a switching device (relay based for example) constitute the high power battery charger. The charging power is limited by the motor thermal limit and inverter limit that means it will be a high power charger in a typical PHEV. Fig. 2 shows a simple schematic diagram of the proposed integrated charger. The motor/generator rotates at the synchronous speed, so as shown in Fig. 2, a second clutch is added to the system to disconnect the motor/generator from the transmission system during the charging.

A. The IPMSM Machine with Split Stator Windings

In a two-pole three-phase IPMSM there are three windings in the stator shifted 120 electrical degrees [5]. Assume that each phase winding is divided into two equivalent parts and moreover they are shifted symmetrically around the stator periphery. Basically there will be six windings inside the stator instead of three for a two pole machine. Fig. 3 shows the cross

978-1-4244-8218-4/10/$26.00 ©2010 IEEE

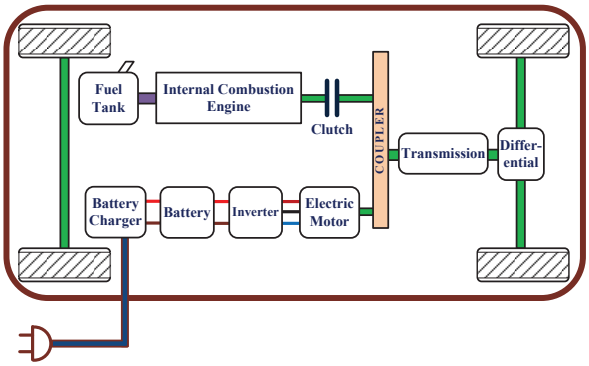

Fig. 1: Simplified schematic diagram of a PHEV

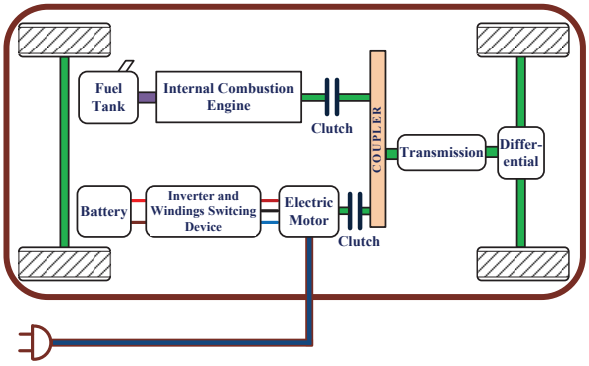

Fig. 2: Simplified schematic diagram of a PHEV using galvanic-isolated integrated charger

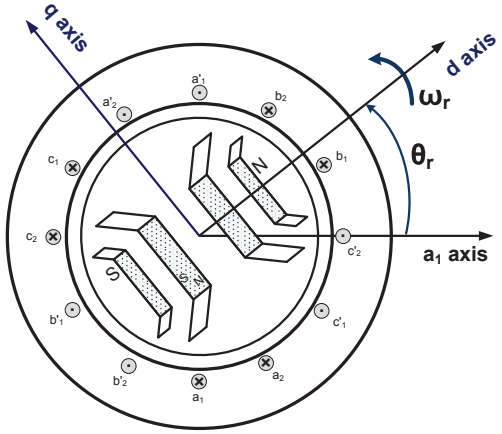

Fig. 3: Cross section of a IPMSM with split stator windings

section of the motor in this configuration. As is shown in this figure, there are six windings shifted 60 electrical degrees while the rotor has a two-pole configuration. Other number of pole pairs are also possible for the machine with this integrated charger.

These six windings can be considered as two sets of three-phase windings. Let say a_1, b_1 and c_1 are the first set of windings (the same as classical three-phase windings). a_2, b_2 and c_2 are the second set of three-phase windings. These two sets of three-phase windings are shifted 30 electrical degrees (angle between magnetic axis of $a_1'a_1$ and $a_2'a_2$) in this configuration.

B. Mathematical Model of the IPMSM with Six Stator Windings

A mathematical model of this machine is developed based on the assumption that all windings magnetomotive force and rotor magnets are sinusoidally distributed. To model this machine with six stator windings, the inductance matrix is first calculated (a 6×6 matrix including self inductances and mutual inductances). Afterwards, the flux and voltage equations are written to model the electrical system [5]. The derivative of the co-energy is calculated to obtain the developed electromagnetic torque. The order of system is eight that is six electrical equations and two mechanical equations in the phase domain. A special abc to dq transformation is used that is based on the Park transformation but an extended version for six variables instead of three. The system equations in the dq frame is reduced to a six order system while all $\sin$ and $\cos$ terms are eliminated from the equations.

If we define the vectors and matrixes for the currents, voltages, flux, inductances and resistance as following:

$$\mathbf{L_s} = \begin{bmatrix} L_{a_1a_1} & L_{a_1b_1} & L_{a_1c_1} & L_{a_1a_2} & L_{a_1b_2} & L_{a_1c_2} \\ L_{b_1a_1} & L_{b_1b_1} & L_{b_1c_1} & L_{b_1a_2} & L_{b_1b_2} & L_{b_1c_2} \\ L_{c_1a_1} & L_{c_1b_1} & L_{c_1c_1} & L_{c_1a_2} & L_{c_1b_2} & L_{c_1c_2} \\ L_{a_2a_1} & L_{a_2b_1} & L_{a_2c_1} & L_{a_2a_2} & L_{a_2b_2} & L_{a_2c_2} \\ L_{b_2a_1} & L_{b_2b_1} & L_{b_2c_1} & L_{b_2a_2} & L_{b_2b_2} & L_{b_2c_2} \\ L_{c_2a_1} & L_{c_2b_1} & L_{c_2c_1} & L_{c_2a_2} & L_{c_2b_2} & L_{c_2c_2} \end{bmatrix},$$

$$\mathbf{i_s} = \begin{bmatrix} i_{a_1} & i_{b_1} & i_{c_1} & i_{a_2} & i_{b_2} & i_{c_2} \end{bmatrix}^T,$$

$$\mathbf{v_s} = \begin{bmatrix} v_{a_1} & v_{b_1} & v_{c_1} & v_{a_2} & v_{b_2} & v_{c_2} \end{bmatrix}^T,$$

$$\psi_\mathbf{s} = \begin{bmatrix} \psi_{a_1} & \psi_{b_1} & \psi_{c_1} & \psi_{a_2} & \psi_{b_2} & \psi_{c_2} \end{bmatrix}^T \text{ and}$$

$$\mathbf{R_s} = \begin{bmatrix} r_s & 0 & 0 & 0 & 0 & 0 \\ 0 & r_s & 0 & 0 & 0 & 0 \\ 0 & 0 & r_s & 0 & 0 & 0 \\ 0 & 0 & 0 & r_s & 0 & 0 \\ 0 & 0 & 0 & 0 & r_s & 0 \\ 0 & 0 & 0 & 0 & 0 & r_s \end{bmatrix}$$

the voltage and flux equations can be written as [5]:

$$\mathbf{v_s} = \mathbf{R_s i_s} + \frac{d}{dt}\psi_\mathbf{s}. \tag{1}$$

v_{a_1}, v_{b_1}, v_{c_1}, v_{a_2}, v_{b_2}, v_{c_2}, i_{a_1}, i_{b_1}, i_{c_1}, i_{a_2}, i_{b_2}, i_{c_2}, ψ_{a_1}, ψ_{b_1}, ψ_{c_1}, ψ_{a_2}, ψ_{b_2}, ψ_{c_2} and r_s are windings voltages, currents, flux linkages and resistance. $L_{a_1a_1}$, $L_{b_1b_1}$, $L_{c_1c_1}$, $L_{a_2a_2}$, $L_{b_2b_2}$ and $L_{c_2c_2}$ are windings self inductances. Moreover, $L_{a_1b_1}$, $L_{a_1c_1}$, $L_{a_1a_2}$, $L_{a_1b_2}$, $L_{a_1c_2}$, $L_{b_1bc_1}$, $L_{b_1c_2}$, $L_{c_1b_2}$, $L_{a_2b_2}$, $L_{a_2c_2}$ and $L_{b_2c_2}$ are windings mutual inductances. θ_r is the angle between rotor d axis and magnetic axes of winding $a_1'a_1$. The inductances are functions of the rotor position θ_r [5].

The developed electromagnetic torque in the machine can be calculated as [5]:

$$T_e = \frac{P}{2}\left(\frac{1}{2}\mathbf{i_s^T}\frac{\partial \mathbf{L_s}}{\partial \theta_r}\mathbf{i_s} + \mathbf{i_s^T}\frac{\partial \psi_\mathbf{pm}}{\partial \theta_r}\right) \tag{2}$$

where P is the machine number of poles. $\psi_{\mathbf{pm}}$ is stator winding fluxes due to rotor magnets. The mechanical dynamical equations describing the machine are:

$$\frac{d\omega_r}{dt} = \frac{P}{2J}(T_e - \frac{2B_m}{P}\omega_r - T_L) \tag{3}$$

$$\frac{d\theta_r}{dt} = \omega_r \tag{4}$$

where J, B_m, T_L and ω_r are the moment of inertia, viscous friction coefficient, load torque and speed of the machine.

To simplify the machine equations a special version of the Park transformation is used to reduced the system order and all sinusoidal terms. The transformation matrix, $\mathbf{K_s}$, is applied to machine equations to transform them to the synchronous dq0 reference frame. This matrix defined as:

$$\mathbf{K_s} = \frac{2}{3}\begin{bmatrix} cos\theta_r & cos(\theta_r - \frac{2\pi}{3}) & cos(\theta_r + \frac{2\pi}{3}) & \dots \\ -sin\theta_r & -sin(\theta_r - \frac{2\pi}{3}) & -sin(\theta_r + \frac{2\pi}{3}) & \dots \\ \frac{1}{2} & \frac{1}{2} & \frac{1}{2} & \dots \\ 0 & 0 & 0 & \dots \\ 0 & 0 & 0 & \dots \\ 0 & 0 & 0 & \dots \end{bmatrix}$$

$$\begin{bmatrix} 0 & 0 & 0 \\ 0 & 0 & 0 \\ 0 & 0 & 0 \\ cos(\theta_r - \frac{\pi}{6}) & cos(\theta_r - \frac{2\pi}{3} - \frac{\pi}{6}) & cos(\theta_r + \frac{2\pi}{3} - \frac{\pi}{6}) \\ -sin(\theta_r - \frac{\pi}{6}) & -sin(\theta_r - \frac{2\pi}{3} - \frac{\pi}{6}) & -sin(\theta_r + \frac{2\pi}{3} - \frac{\pi}{6}) \\ \frac{1}{2} & \frac{1}{2} & \frac{1}{2} \end{bmatrix}$$

By transforming the phase variables to the rotor reference frame by applying the transformation matrix $\mathbf{K_s}$, the machine equations will be simplified with reduced number of equations. In the rotor reference frame the variables are superscripted by letter r and are defined as:

$$\mathbf{i_s^r} = \begin{bmatrix} i_{d_1} & i_{q_1} & i_{0_1} & i_{d_2} & i_{q_2} & i_{0_2} \end{bmatrix}^T,$$

$$\mathbf{v_s^r} = \begin{bmatrix} v_{d_1} & v_{q_1} & v_{0_1} & v_{d_2} & v_{q_2} & v_{0_2} \end{bmatrix}^T \textit{and}$$

$$\psi_{\mathbf{s}}^{\mathbf{r}} = \begin{bmatrix} \psi_{d_1} & \psi_{q_1} & \psi_{0_1} & \psi_{d_2} & \psi_{q_2} & \psi_{0_2} \end{bmatrix}^T.$$

The indexes d, q and 0 denote the direct axis, quadrature axis and zero component of the variables. Moreover, there are two set of three-phase quantities that are denoted by the numbers 1 and 2 respectively. For example the voltage can be transformed from the abc domain to the dq domain by $\mathbf{v_s^r} = \mathbf{K_s v_s}$.

By transforming machine voltage, flux linkage and torque equations to the dq reference frame, the following equations describe the dynamical model [6]:

$$v_{d_1} = r_s i_{d_1} + \frac{d}{dt}\psi_{d_1} - \omega_r \psi_{q_1} \tag{5}$$

$$v_{q_1} = r_s i_{q_1} + \frac{d}{dt}\psi_{q_1} + \omega_r \psi_{d_1} \tag{6}$$

$$v_{d_2} = r_s i_{d_2} + \frac{d}{dt}\psi_{d_2} - \omega_r \psi_{q_2} \tag{7}$$

$$v_{q_2} = r_s i_{q_2} + \frac{d}{dt}\psi_{q_2} + \omega_r \psi_{d_2} \tag{8}$$

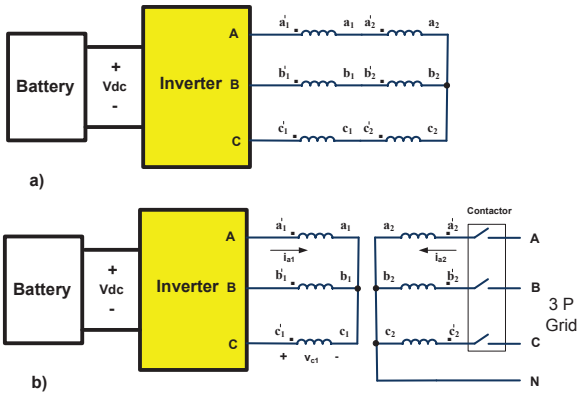

Fig. 4: System modes of operation: a) traction and b) charging

$$\psi_{d_1} = L_d i_{d_1} + L_{md} i_{d_2} + \psi_{pm} \tag{9}$$

$$\psi_{q_1} = L_q i_{q_1} + L_{mq} i_{q_2} \tag{10}$$

$$\psi_{d_2} = L_{md} i_{d_1} + L_d i_{d_2} + \psi_{pm} \tag{11}$$

$$\psi_{q_2} = L_{mq} i_{q_1} + L_q i_{q_2} \tag{12}$$

where L_d, L_q, L_{md}, L_{mq} are direct and quadrature axis winding self and mutual inductances respectively. Moreover, $L_d = L_l + L_{md}$ and $L_q = L_l + L_{mq}$. It is assumed that the zero components are zero due to symmetrical three-phase quantities.

The developed electromagnetic torque can be expressed as [6]:

$$T_e = \frac{3}{2}\frac{P}{2}[\psi_{pm}(i_{q_1}+i_{q_2})+(L_d-L_q)(i_{d_1}i_{q_1}+i_{d_1}i_{q_2}+i_{d_2}i_{q_1}+i_{d_2}i_{q_2}]. \tag{13}$$

III. System Modes of Operation: Traction and Charging

As mentioned before, the system has two modes of operation: traction and charging. In the traction mode, each two windings are connected to each other in series to constitute a three-phase winding set. These three windings can be connected to each other in Δ or Y to form a classical three-phase machine. Moreover, the motor is powered by the battery through the inverter. Fig. 4.a shows the system diagram in this mode. Sensorless schemes for example can be employed to run the motor in the traction mode [7].

For the charging mode the system is reconfigured according to the scheme shown in Fig. 4.b. A simple relay based device can re-connect the windings and a contactor is needed to connect the system to the utility grid.

In the proposed integrated charger, if the machine would be kept in standstill as in [8], the magnetization current will be high due to large the air-gap. So it is expected to have lower system efficiency depending on the air-gap length. However, if the machine rotates with the grid synchronous speed, the magnets will induce voltages in the inverter-side windings that emulates an isolated PM ac generator for the inverter. The idea is thus to connect the machine to the grid via the grid-side

three-phase windings, a_2, b_2 and c_2. These three windings can be used to run the machine as a classical motor. The inverter side windings, a_1, b_1 and c_1 will pick up the induced voltage due to the developed flux inside the machine (since they are located on the same pole-pair of the grid-side windings). The inverter can use this isolated voltage source to charge the battery by the means of machine leakage inductances as the converter energy storage component (three-phase boost converter).

To synchronize the machine to the grid, the inverter will run the motor by the means of the battery through the windings a_1, b_1 and c_1. The other windings are open circuited (contactor is open) but the induced voltage will be measured to be synchronized with the grid voltage. When the grid-side winding voltages are synchronized with the grid, the contactor will be closed and the grid voltage will be applied to the grid-side windings. Afterwards, the inverter will control the inverter side winding voltages to charge the battery which is called charge control here.

A. Motor/Generator Grid Synchronization

The machine windings will be reconfigured by a switching device, like relays, before start of the charge. After this operation the machine is still in standstill (the vehicle is parked during the charging). A contactor is used to connect the grid-side windings to the grid. Before connection to the grid, the machine must be rotated at the synchronous speed and produce the same voltage as the grid does (both amplitude and phase) for the safe grid connection. This process is called grid synchronization for the proposed integrated charger.

At first, the inverter-side windings is used to drive the motor by the means of the battery and proper inverter operation while the grid-side windings are open connected. Before closing the contactor, dc link voltages, motor/genereator primary side currents and rotor position/speed are measured to have a classical field oriented speed control for the IPM motor [9]. The position/speed can be estimated instead of using a sensor, but here for simplicity it is assumed that the position and speed signals are available.

Both grid-side winding voltages, and grid voltages are measured and transformed to the $\alpha\beta$ reference frame. Both voltage vectors magnitude and angle of the grid voltage and motor/generator grid-side windings should be equal as an index of synchronization. The magnitude of voltage is a function of the motor speed and flux (refer to motor/generator equations), so by controlling the flux, the voltage level can be adjusted. In a classical IPM motor usually the reference value for the d component of the machine is zero (for flux weakening operation this value will be modified), but at this scheme this value is used as a control parameter to change the induced voltage magnitude.

The motor/generator will rotate at the synchronous speed to meet the frequency synchronization requirement. So the speed reference will be $2\pi 50 rad/sec$ for a grid with $50Hz$ frequency supply. Moreover, to match the voltage angles, a PI controller is used to adjust the motor/generator speed reference due to the angle error signal. This speed reference will be tracked by the field oriented speed control part of the system.

After the synchronization, both voltage magnitude and angle error signals are small values within predefined bands, the motor/generator set is synchronized and the contactor will be closed. Now the system is ready for the charge operation.

B. Battery Charge Control

Fig. 5 shows a basic diagram of a three-phase boost converter. This scheme is very similar to the proposed integrated charger system. The voltage equations describing the converter in the dq reference frame are [4]:

$$u_{Ld} = Ri_{Ld} + L\frac{d}{dt}i_{Ld} - \omega i_{Lq} + u_{Id} \tag{14}$$

$$u_{Lq} = Ri_{Lq} + L\frac{d}{dt}i_{Lq} - \omega i_{Ld} + u_{Iq} \tag{15}$$

where u_{Ld}, u_{Lq}, u_{Id} and u_{Iq} are line and inverter dq voltage components respectively. R, L and ω are the resistance, inductance and source frequency also. As is shown in the figure i_{Ld} and i_{Lq} are d an q components of the line currents. The active and reactive power going inside the converter can be written as [4]:

$$p = \frac{3}{2}(u_{Ld}i_{Ld} + u_{Lq}i_{Lq}) \tag{16}$$

$$q = \frac{3}{2}(u_{Lq}i_{Ld} - u_{Ld}i_{Lq}) \tag{17}$$

Different control strategies have been proposed for this three-phase boost converter operation [4]. If $i_{Lq} = 0$ and $u_{Lq} = 0$ in the equations above, then the active and reactive power will be simplified to $p = \frac{3}{2}u_{Ld}i_{Ld}$ and $q = 0$. Based on these equations, the feedforward current control method is one of the widely used schemes for power control. Fig. 6 shows the basic diagram of the controller. dq current control and feeforward compensation are main parts of this decoupled control scheme. The controller has an outer loop for the dc bus voltage regulation. This controller output sets the reference value for the d component of the current that will control the power. Two independent PI controller have been used to generate reference values for the converter, u_α and u_β. The feedforward terms will be added to this reference values to the decouple system in d and q axes to improve the system performance.

For the proposed integrated charger, after grid synchronization the contactor will be closed and the grid voltages will be applied to the grid-side motor/generator windings. It will be a constant voltage source for the windings. The motor/generator voltage equations can be written as below after some mathematical manipulations [6]:

$$v_{d_2} = r_s(i_{d_2} - i_{d_1}) + L_l\frac{d}{dt}(i_{d_2} - i_{d_1}) - \omega_r L_l(i_{d_2} - i_{d_1}) + v_{d_1} \tag{18}$$

$$v_{q_2} = r_s(i_{q_2} - i_{q_1}) + L_l\frac{d}{dt}(i_{q_2} - i_{q_1}) + \omega_r L_l(i_{q_2} - i_{q_1}) + v_{q_1}. \tag{19}$$

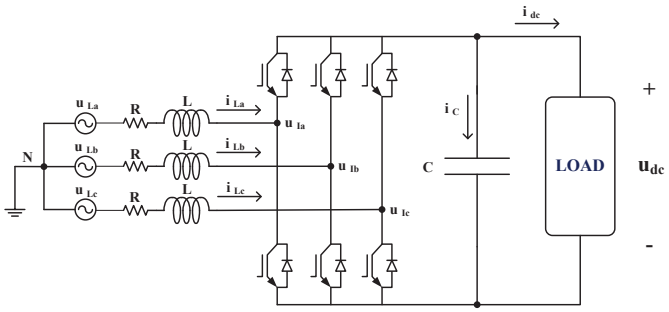

Fig. 5: The power stage of the three-phase boost converter

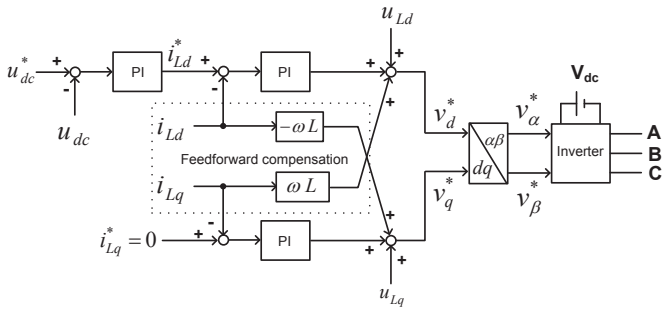

Fig. 6: Decoupled current control of the three-phase boost converter

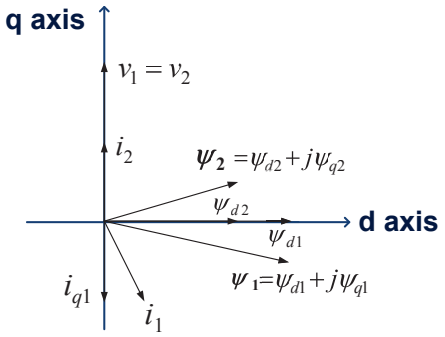

Fig. 7: Motor/generator vector diagram in the charging mode

The equations above are very similar to equations 14 and 15 that describe the classical three-phase boost converter. The difference is that currents are replaced by the difference of the primary and secondary winding currents. So the same control strategy is adopted with small modifications (adjusting the currents by the current differences). Moreover, due to existence of a battery in the dc link, the dc bus voltage controller is eliminated from the scheme. With assumption of the symmetrical three-phase currents and voltages for the inverter-side and grid-side windings, each three-phase quantity can be represented by a classical two-dimensional vector with the extended dq transformation (there is no coupling in the matrix transformation between the two systems). Fig. 7 shows the motor/generator vector diagram in steady state operation for the charging mode (assume that controllers are tuned). The grid voltage is in the q direction and the grid current just has a q component to achieve unit power factor operation from the grid point of view. The inverter-side current is in opposite direction of the grid side current. There is a small d component current to adjust the machine voltage level (proportional to speed and machine flux).

The system has a bidirectional power flow capability that is inherent in the system because of the bidirectional operation of the three-phase inverter. Moreover, by changing the set point of the d component of the current, there is a possibility of production/generation of the reactive power also. The system power limitation is mainly a thermal limitation of the machine in the classical vehicle drive systems. Half of the machine's full power can be used in the charging mode (the converter withstand this power level because it is designed for machine full power operation).

IV. Simulation Results

The whole system has been simulated by the use of Matlab/Simulink software based on the before mentioned system equations. The ideal converter is used in the simulation (no PWM or SVM is used for the inverter). The motor parameters used in the simulation (as a typical example) are shown in Table I.

It is assumed that the system is reconfigured for the charging operation (refer to Fig 4.b) but the grid contactor is open firstly. The inverter will start to rotate the motor by the means of the battery and motor inverter side windings (a_1, b_1 and c_1) to synchronize the grid-side windings ((a_2, b_2 and c_2) voltages to the grid voltage. The motor will rotate at the grid synchronous speed. Afterwards, the motor voltages and grid voltages are compared to each other in the $\alpha\beta$ reference frame. After 20 seconds the synchronization will be finished (it can be faster) and the contactor is closed. For 5 seconds the system will stay synchronized and then the charge control is started. So the charge control is started after 25 seconds.

Fig. 8 shows the motor/generator winding voltages for phase a during synchronization. The windings are shifted $\pi/6$ electrical degrees in the stator periphery and this leads to a voltage shift in the grid-side and inverter-side windings that can be identified from the figure. The grid power to the charger is shown in Fig. 9. The power is negative before start of the charging meaning the inverter is powering the system through the battery. The rotor electrical speed is shown in Fig. 10. There are some oscillations in the rotor that the controller adjusts. Fig. 11 shows line currents (grid current) after closing the contactor. After synchronization and closing the contactor, the grid voltage will be applied to the grid-side windings. A small amount of current is needed in the machine to keep the machine synchronized with the grid.

The machine stator resistance are the single loss generating component in the whole simulation, so it is expected to have high efficiency. The system efficiency is more than 92% for this small machine. For an accurately designed system the efficiency will be higher.

V. Conclusion

An innovative integrated charger has been presented for PHEV applications based on a special IPM machine. The

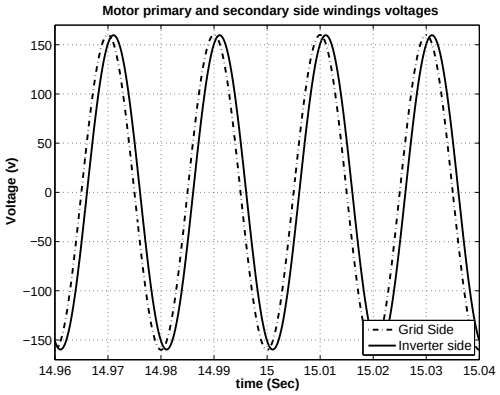

Fig. 8: Motor/generator shifted winding voltages in the charging mode

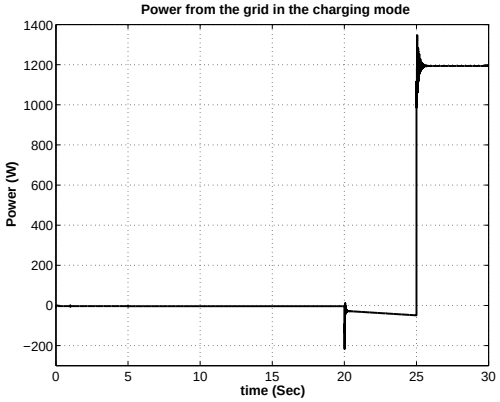

Fig. 9: Grid power to the charger system

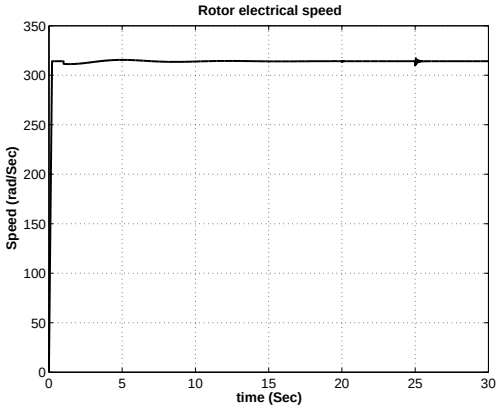

Fig. 10: Electrical speed of the motor/generator

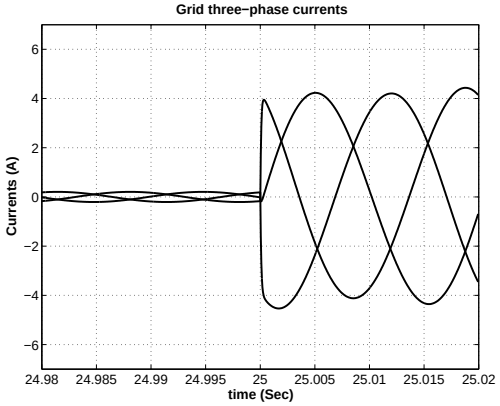

Fig. 11: Three-phase line currents (grid-side) of the motor/generator

TABLE I: IPM MOTOR PARAMETRS

Rated power (kW)	2.2
Rated line voltage (V)	380
Rated current (A)	4.1
Rated speed(rev/min)	1750
No of poles	6
Permanent magnet flux (Wb)	0.48
Stator resistance (Ohm)	0.66
d axis inductance (mH)	42
q axis inductance (mH)	57
Inertia (Kg.m2)	0.01
Viscous friction coefficient (Nms/rad)	0.002

charger is a high-power bi-directional fast charger with unit power factor. Moreover, it is galvanically isolated that make it a favorite solution for safety reasons. The system configuration for traction and charging are described. The mathematical model of the machine in the charging mode including six windings in the stator is presented. The system has two modes of operation: traction and charging. The system functionality is described for the charging mode. In charging mode before grid connection, the motor/generator is synchronized and afterwards the charge control is started. Some simulation results are presented to exemplify the system operation.

ACKNOWLEDGMENT

The authors would like to thank Swedish Hybrid Vehicle Center (SHC) for financing the project and support.

REFERENCES

[1] Saeid Haghbin, Kashif Khan, Sonja Lundmark, Mats Alakula, Ola Carlson, Mats Leksell and Oskar Wallmark, "Integrated Chargers for EVs and PHEVs: Examples and New Solutions," To be published in International Conference on Electrical Machines (ICEM) proceedings, 2010, Italy.

[2] Kashif Khan, Saeid Haghbin, Mats Leksell and Oskar Wallmark, "Design and Performance Analysis of Permanent-Magnet Assisted Synchronous Reluctance Machines for Integrated Charger," To be published in International Conference on Electrical Machines (ICEM) proceedings, 2010, Italy.

[3] A. Emadi, Young Joo Lee, K. Rajashekara, "Power Electronics and Motor Drives in Electric, Hybrid Electric, and Plug-In Hybrid Electric Vehicles," IEEE Transactions on Industrial Electronics, vol.55, no.6, pp.2237-2245, June 2008.

[4] M. Malinowski, "Sensorless control strategies for three-phase PWM rectifiers," Ph.D. Thesis, Warsaw Univ. of Technology, Poland, 2001.

[5] Sergey Edward Lyshevski, "Electromechanical Systems, Electric Machines, and Applied Mechatronics," CRC Press, 1999.

[6] Saeid Haghbin, "Integrated charger for plug-in hybrid electric vehicles," Licentiate Thesis, Chalmers University of Technology, to be published in 2010.

[7] Peter Vas, "Sensorless vector and direct torque control," Oxford Press, 1998.

[8] F. Lacressonniere and B. Cassoret, "Converter used as a battery charger and a motor speed controller in an industrial truck," European Conference on Power Electronics and Applications, 2005.

[9] Bimal K. Bose, "Modern power electronics and ac drives," Prentice Hall, 2001.